



HTR-N & N1
High-Temperature Reactor Physics and Fuel Cycle Studies
(EC-funded Projects: FIKI-CT-2000-00020 & FIKI-CT-2001-00169)

Work Package: 1	HTR-N project document No.: HTR-N-02/09-S-1.1.2				Q.A. level: 1
Task: 1.1&1.2	Document type: EC deliverable				Document status: final
Issued by: NRG	original document No.: ECN-I-98-056.doc	Annex pg. 17	Rev. 1	Q.A. level A	Dissemination level: RE

Document Title

ANALYSIS OF THE HTTR WITH MONTE-CARLO AND DIFFUSION THEORY

Author(s)

J.B.M. de Haas and E.J.M. Wallerbos*

Organisation, Country

NRG, The Netherlands
*IRI, Delft University of Technology

Notes

Electronic filing:

Electronic file format:

SINTER

Microsoft Word 97

1	12 09 03	Final version	JL			Z
0	12 09 02	first issue	NRG J. de Haas	CEA, FZJ	CEA X. Raepsaet	FZJ W. von Lensa
Rev.	Date	Short Description	Prepared by	Partners' Review	Control WP Manager	Approval Project Manager

confidential information property of the HTR-N project - not to be used for any purpose other than that for which is supplied

Work Package: 1	HTR-N project document No.: HTR-N-02/09-S-1.1.2	Rev. 1
Task: 1.1&1.2	Document type: EC deliverable	

Chronology and history of revisions

Rev.	Date	Description
0	12-09-02	First issue forbHTR-N Partners Comments
1	12 09 03	Final version

Work Package: 1	HTR-N project document No.: HTR-N-02/09-S-1.1.2	Rev. 1
Task: 1.1&1.2	Document type: EC deliverable	

SEPTEMBER 1998

ECN--I-98-056

ANALYSIS OF THE HTTR WITH MONTE-CARLO AND DIFFUSION THEORY

An IRI, ECN intercomparison

J.B.M. de Haas and E.J.M. Wallerbos*

*Interfaculty Reactor Institute (IRI), Delft University of Technology

author : J.B.M. de Haas

reviewed : J.L. Kloosterman (IRI)

21415/RE/JdH/AK/22181

approved : A.I. van Heek

Work Package: 1	HTR-N project document No.: HTR-N-02/09-S-1.1.2	Rev. 1
Task: 1.1&1.2	Document type: EC deliverable	

SUMMARY

In the framework of the IAEA Co-ordinated Research Program (CRP) “Evaluation of HTGR Performance” for the start-up core physics benchmark of the High Temperature Engineering Test Reactor (HTTR) two-group cross section data for a fuel compact lattice and for a two-dimensional R-Z model have been generated for comparison purposes. For this comparison, 5.2% enriched uranium was selected. Furthermore, a simplified core configuration utilising only the selected type of fuel has been analysed with both the Monte Carlo code KENO and with the diffusion theory codes BOLD VENTURE and PANTHER.

With a very detailed KENO model of this simplified core, k_{eff} was calculated to be 1.1278 ± 0.0005 . Homogenisation of the core region was seen to increase k_{eff} by 0.0340 which can be attributed to streaming of neutrons in the detailed model. The difference in k_{eff} between the homogenised models of KENO and BOLD VENTURE amounts then only $\Delta k = 0.0025$.

The PANTHER result for this core is $k_{\text{eff}} = 1.1251$, which is in good agreement with the KENO result.

The fully loaded core configuration, with a range of enrichments, has also been analysed with both KENO and BOLD VENTURE. In this case the homogenisation was seen to increase k_{eff} by 0.0375 (streaming effect). In BOLD VENTURE the critical state could be reached by the insertion of the control rods through adding an effective ^{10}B density over the insertion depth while the streaming of neutrons was accounted for by adjustment of the diffusion coefficient.

The generation time and the effective fraction of delayed neutrons in the critical state have been calculated to be 1.11 ms and 0.705%, respectively. This yields a prompt decay constant at critical of 6.9 s^{-1} .

The analysis with PANTHER resulted in a $k_{\text{eff}} = 1.1595$ and a critical control rod setting of 244.5 cm compared to the detailed KENO results of: $k_{\text{eff}} = 1.1600$ and 234.5 cm, again an excellent agreement.

Work Package: 1	HTR-N project document No.: HTR-N-02/09-S-1.1.2	Rev. 1
Task: 1.1&1.2	Document type: EC deliverable	

CONTENTS

1. INTRODUCTION	7
2. CROSS SECTION GENERATION	9
2.1 Cross sections for the use in KENO	9
2.1.1 Procedure	9
2.1.2 Two-group cross sections	10
2.2 Cross sections for BOLD-VENTURE	12
2.2.1 Procedure	12
2.2.2 Two-group cross sections	13
2.3 Cross sections for PANTHER	15
2.3.1 General	15
2.3.2 PROCOL	16
2.3.3 PIJ	17
3. ANALYSIS OF THE SIMPLE CORE WITH KENO	19
3.1 Model of the HTTR	19
3.2 Results	19
4. ANALYSES OF THE SIMPLE CORE WITH BOLD-VENTURE	20
4.1 Model of the HTTR	20
4.2 Results	20
5. ANALYSIS OF THE SIMPLE CORE WITH PANTHER	21
5.1 Model of the HTTR	21
5.2 Results	21
6. ANALYSIS OF THE FULLY LOADED CORE WITH BOLD-VENTURE	22
6.1 Model of the HTTR	22
6.2 Results	22
7. ANALYSIS OF THE FULLY LOADED CORE WITH PANTHER	25
7.1 Model of the HTTR	25
7.2 Results	25
8. CONCLUSION	27
9. REFERENCES	28
10. FIGURES	29
APPENDIX	43
1 Atomic densities in the homogenised model.	43
1.1 The simple core	44
1.2 The fully loaded core	44

HTR-N

Work Package: 1	HTR-N project document No.: HTR-N-02/09-S-1.1.2	Rev. 1
Task: 1.1&1.2	Document type: EC deliverable	

Work Package: 1	HTR-N project document No.: HTR-N-02/09-S-1.1.2	Rev. 1
Task: 1.1&1.2	Document type: EC deliverable	

INTRODUCTION

Both ECN and IRI take part in the benchmark of start-up core physics of the High Temperature Engineering Test Reactor (HTTR), which is described in detail in Ref. 1, and is part of the IAEA Co-ordinated Program “Evaluation of HTGR Performance The IRI results obtained with Monte Carlo techniques for the problems in this benchmark are described elsewhere [2]. Because the configuration of the core is quite complicated with in total 12 different uranium enrichments, ECN and IRI decided to analyse a simpler configuration also, and compare cross sections and the core model. In this simpler configuration only 5.2 % enriched uranium is used for all fuel blocks in the reactor (the fuel block in layer 5, zone 2, see ref. 1). For the comparison of cross sections, it was agreed to condense the energy range into two groups with the boundary at 2.1 eV.

This report first describes the generation of cross sections for both Monte Carlo calculations and for calculations with deterministic codes. Subsequently, results of the analysis of the simple core configuration with the multi-group Monte Carlo code KENO and the diffusion theory codes BOLD VENTURE and PANTHER are presented. Then results obtained with BOLD VENTURE are given for the fully loaded core which has a variety on enrichments in the fuel assemblies. This includes the generation time and the effective fraction of delayed neutrons at critical. Finally, results for the fully loaded core with PANTHER are presented.

HTR-N

Work Package: 1	HTR-N project document No.: HTR-N-02/09-S-1.1.2	Rev. 1
Task: 1.1&1.2	Document type: EC deliverable	

Work Package: 1	HTR-N project document No.: HTR-N-02/09-S-1.1.2	Rev. 1
Task: 1.1&1.2	Document type: EC deliverable	

CROSS SECTION GENERATION

The computational tools used at IRI for the cross section generation have been described previously [2]. In short it contains, as a branch, the SCALE-4 code system with master libraries produced by NJOY from the JEF-2.2 basic nuclear data files. The used reactor codes for this study are: KENO-Va and BOLD VENTURE.

At ECN the WIMS-7B code system has been used for this study which has libraries also based on JEF-2.2. The reactor code used at ECN is PANTHER-5.0.

Cross sections for the use in KENO

In KENO, only the coated fuel particles (CFP's) in the fuel compacts are homogenised with the graphite matrix of the fuel compacts; all other reactor components can be modelled explicitly. As the fuel also contains the only two resonant nuclides (^{235}U and ^{238}U) present in the core model, the only problem is the generation of cross sections for the homogenised fuel compacts.

The general CFP and compact data are:

	radius (μm)	density (g/cm^3)	material
fuel kernel	298.5	10.79	UO_2
1st coating	358.5	1.14	PyC (low dens.)
2nd coating	389.5	1.89	PyC
3rd coating	418.5	3.20	SiC
4th coating	464.5	1.87	PyC

PyC: Pyrolytic graphite

Compact dimensions: i/o diameter = 1.00/2.60 cm, height = 3.91 cm.

Procedure

Since the problem is similar to the generation of cross sections for the fuel pebbles of a pebble-bed type HTR, the following scheme was adopted from the analysis work for HTR-PROTEUS [2]:

1. First only the coated fuel particles inside a fuel rod are considered. An infinite close-packed hexagonal CFP lattice is calculated by BONAMI, NITAWL and XSDRNPM. XSDRNPM is run in spherical geometry for a white boundary elementary cell of the CFP lattice. This elementary cell contains two regions: a sphere of 0.0597 cm diameter which contains the fuel kernel of UO_2 surrounded by the homogenised mixture of the coating layers and graphite matrix in the fuel compact. The matrix graphite contains some natural boron to represent impurities in the graphite. A cell-averaged weighted library, WGH(1), is produced which takes the self-shielding of the fuel in the Caps into account.
2. An infinite fuel-rod lattice is treated by BONAMI and NITAWL to obtain working library WRK(1). The unit cell with cylinder geometry has three regions. The innermost region is a channel filled with helium (0.5 cm radius). This region is surrounded by a cylinder of 1.3 cm radius with the fuel. The outermost region surrounding the fuel contains fuel block graphite ($r = 3.29$ cm). A triangular lattice is assumed with a pitch of 6.2668 cm, consistent with 1/33rd block for the 33-rods fuel

Work Package: 1	HTR-N project document No.: HTR-N-02/09-S-1.1.2	Rev. 1
Task: 1.1&1.2	Document type: EC deliverable	

block. This step is required because it provides the unweighted data for the materials outside the fuel region. The overall Dancoff factor for the core has been deduced from the Dancoff factors for a lattice of CFP's in a fuel compact and for a lattice of fuel rods in a fuel block [2].

3. The library WRK(1) cannot be used for the fuel-rod lattice cell calculation as it would not take into account the self-shielding in the CFP's. Therefore the WGH(1) and WRK(1) libraries are merged. All fuel-region materials are taken from the weighted library WGH(1), the other materials from WRK(1). The resulting library is called WRK(2).
4. XSDRNPM is run with working library WRK(2) for the unit cell of the infinite fuel-rod lattice. This unit cell of cylindrical geometry has five radial zones: 1. Channel with helium ($r \leq 0.5$ cm). 2. Fuel zone ($r \leq 1.3$ cm). 3. Graphite sleeve of fuel rod ($r \leq 1.7$ cm). 4. Fuel hole in fuel block filled with helium ($r \leq 2.05$ cm). 5. Fuel block graphite with reduced density to take the fuel handling hole into account. The radius is of this zone is 3.2903 cm (1/33rd fuel block). If no axial dimensions are used, this run yields the k_{∞} of the fuel rod lattice. XSDRNPM is run with a buckling search option to get a critical system (by the addition of a leakage term in the form of $DB^2\phi$). The weighted library WGH(2) with **zone**-averaged cross sections is produced.
5. In order to obtain a working library for KENO, WGH(2) and WRK(1) are merged. The cross sections for the nuclides inside the fuel compact are taken from WGH(2), and the cross sections for all nuclides in the other components (He, C, ^{10}B , and ^{11}B) are taken from WRK(1). The resulting library is denoted as WRK(3).

No group collapsing is done in any of these steps. All libraries contain cross section data for 172 energy groups! A simpler scheme would have been possible if no comparison had to be made for two-groups cross sections.

Two-group cross sections

In total, five two-group cross-section libraries have been generated for comparison purposes:

1. GRLAT2GR: XSDRNPM output of step 1 but with condensation
2. RODLAT_K: output of XSDRNPM k-calculation using WRK(1) as input (step 2)
3. HTTR_K: output of step 4 XSDRNPM, k-calculation and using WRK(2) as input
4. HTTR_B2: output of step 4 XSDRNPM, buckling search using WRK(2) as input
5. RODLAT_B2: output of XSDRNPM, buckling search and using WRK(1) as input (step 2)

The order of the numbers in tables 1 and 2 correspond to this order. These five sets enable the assessment of the effects of step 1, the separate treatment for the coated particles, and of the spectrum used for weighing (buckling search versus k-calculation). Table 1 lists the microscopic total (MT=1), absorption (MT=27), and transport (MT=1000) cross section for the nuclides in the fuel compact. For the uranium isotopes ^{235}U and ^{238}U also the total number of fission neutrons (MT=452), and the fission (MT=18) and capture (MT=101) cross-section are specified in table 2.

Table 1. Two-group cross sections for nuclides in the fuel compact (5.2 w% enrichment)

nuclide	σ_{tot} (b)		σ_{abs} (b)		σ_{tr} (b)	
	group 1	group 2	group 1	group 2	group 1	group 2
¹⁰ B	26.86	1132.4	24.49	1130.3	39.62	1446.0
	47.49	2147.2	45.16	2145.0	34.45	3074.8
	49.40	2157.8	47.07	2155.6	29.67	3080.0
	45.26	2095.3	42.92	2093.2	34.56	2214.5
	44.19	2096.0	41.85	2093.8	34.59	2246.6
¹¹ B	4.239	4.871	6.414 E-5	1.620 E-3	2.796	3.970
	4.267	4.941	8.961 E-5	3.073 E-3	2.686	4.757
	4.274	4.945	9.209 E-5	3.088 E-3	2.608	4.762
	4.223	4.941	8.706 E-5	2.999 E-3	3.441	4.666
	4.225	4.937	8.562 E-5	3.000 E-3	3.436	4.666
C	4.128	4.752	1.295 E-4	1.000 E-3	2.808	3.988
	4.157	4.805	1.567 E-4	1.891 E-3	2.693	4.857
	4.164	4.808	1.576 E-4	1.900 E-3	2.617	4.862
	4.114	4.805	1.673 E-4	1.845 E-3	3.373	4.727
	4.116	4.803	1.647 E-4	1.846 E-3	3.369	4.729
O	3.754	3.889	1.231 E-3	5.561 E-5	7.760	9.647
	3.752	3.943	1.293 E-3	1.062 E-4	2.701	3.840
	3.751	3.912	1.295 E-3	1.054 E-4	2.654	3.794
	3.736	3.910	1.437 E-3	1.023 E-4	3.189	3.757
	3.740	2.941	1.407 E-3	1.036 E-4	3.185	3.790
Si	2.669	2.113	2.644 E-3	5.057 E-2	2.050	1.807
	2.612	2.176	3.548 E-3	9.593 E-2	2.382	2.187
	2.605	2.178	3.621 E-3	9.640 E-2	2.399	2.190
	2.652	2.174	3.570 E-3	9.361 E-2	2.356	2.133
	2.651	2.173	3.511 E-3	9.363 E-2	2.353	2.134
²³⁵ U	22.93	177.5	12.52	163.2	88.03	733.5
	28.80	366.3	18.20	351.5	22.22	543.2
	29.00	363.6	18.39	349.0	19.18	534.0
	27.53	352.2	17.08	337.6	21.45	374.3
	27.60	356.8	17.12	342.1	21.96	385.8
²³⁸ U	14.77	10.08	1.775	0.853	64.94	26.97
	17.71	10.87	3.779	1.545	22.11	11.52
	15.86	10.79	2.879	1.534	14.31	11.38
	15.47	10.75	2.670	1.492	12.65	10.79
	17.27	10.84	3.541	1.510	15.24	10.92

Table 2. Total fission neutrons and fission and capture cross section of uranium isotopes

nuclide	ν		σ_{fis} (b)		σ_{capt} (b)	
	group 1	group 2	group 1	group 2	group 1	group 2
²³⁵ U	2.440	2.439	8.457	137.8	4.066	25.42
	2.437	2.438	11.82	299.9	6.378	51.63
	2.437	2.438	11.92	297.7	6.462	51.25
	2.438	2.438	11.12	288.0	5.962	49.67
	2.438	2.438	11.16	291.8	5.967	50.31
²³⁸ U	2.736	2.489	4.581 E-2	3.577 E-6	1.729	0.853
	2.740	2.489	4.628 E-2	6.640 E-6	3.732	1.545
	2.741	2.489	4.610 E-2	6.591 E-6	2.833	1.534
	2.742	2.489	5.093 E-2	6.407 E-6	2.619	1.492
	2.741	2.489	5.023 E-2	6.486 E-6	3.491	1.510

The spectrum in the grain lattice is much harder than in the fuel-rod lattice, which explains the lower values of the cross sections. The extra leakage term in the buckling search is seen to slightly reduce the cross sections, because of the greater leakage of low energy neutrons compared to high energy neutrons.

Figure 1 shows the spectrum in the centre of the fuel-rod lattice, as calculated with step 4 of the cross-section generation procedure.

Cross sections for BOLD-VENTURE

In BOLD VENTURE the core region is represented by five rings, containing the A, B, C, D, and E labelled columns (see Ref. 1), respectively. The material in each ring is completely homogenised. In order to maintain the reaction rates, the cross-section generation procedure for KENO was extended.

Procedure

The first three steps are identical to the procedure for KENO. The fourth step is similar, but now a **cell** weighting is performed instead of a **zone** weighting. Subsequent steps are new.

1. See page 7 step 1.
2. Idem step 2.
3. Page 8 step 3.
4. XSDRNPM is run with working library WRK(2) for the unit cell of the infinite fuel-rod lattice. This unit cell of cylindrical geometry has five radial zones: 1. Channel with helium ($r \leq 0.5$ cm). 2. Fuel zone ($r \leq 1.3$ cm). 3. Graphite sleeve of fuel rod ($r \leq 1.7$ cm). 4. Fuel hole in fuel block filled with helium ($r \leq 2.05$ cm). 5. Fuel block graphite with reduced density to take the fuel handling hole into account. The burnable poison rods are not taken into account. The radius of this zone is 3.2903 cm (1/33rd fuel block). XSDRNPM is run with a buckling search option to get a critical system (by the addition of a leakage term in the form of $DB^2\phi$). The weighted library WGH(2) with **cell**-averaged cross sections is produced.
5. Unweighted cross sections for the materials outside the fuel blocks (i.e. inside the control rod guide blocks and reflector) have to be added to WGH(2). These

Work Package: 1	HTR-N project document No.: HTR-N-02/09-S-1.1.2	Rev. 1
Task: 1.1&1.2	Document type: EC deliverable	

unweighted cross sections of C, ^{10}B , and ^{11}B , were taken from WRK(1). The resulting library is called WRK(3).

6. XSDRNPM is run with library WRK(3) for a 1D-model of the reactor. This model contains six radial zones. The first five represent the five rings of the core region, the outermost zone represents the permanent reflector. The radii of the zones were calculated to be 19.0064 cm, 50.2861 cm, 82.8468 cm, 115.6112 cm, 148.4444 cm, and 214.9814 cm. With these radii, the area of the rings is identical to the true area of the columns (the pitch in the core region is taken to be 18.1 cm, hence the space between the blocks is taken into account). The material within each zone is completely homogenised. The atomic densities in the homogenised zones can be found in the appendix. Note that the burnable poison rods are not taken into account. XSDRNPM is run with a buckling search option and with zone weighting, producing weighted library WGH(3). For the homogenised KENO model the 172 groups were not condensed, for BOLD VENTURE the groups were condensed to 13 broad groups, like for HTR-PROTEUS [3].

Two-group cross sections

Two-group cross section data is obtained by condensing the 172 fine groups to 2 broad groups in step 6 of the procedure in section 2.2.1.

The results are summarised in tables 3 - 6.

Table 3. Two-group cross sections for the uranium isotopes in the fuel compact (5.2 w% enrichment) in the radial zones B, C, and D.

	σ_{tot} (b)		σ_{abs} (b)		σ_{tr} (b)		
	group 1	group 2	group 1	group 2	group 1	group 2	
^{235}U	B	27.79	368.3	17.18	354.2	21.30	372.4
	C	29.13	378.6	18.39	364.5	23.47	372.8
	D	27.34	380.8	16.78	366.7	21.04	385.3
^{238}U	B	15.71	10.47	2.716	1.544	12.34	10.45
	C	16.08	10.50	2.929	1.581	12.11	10.45
	D	15.59	10.50	2.651	1.589	12.26	10.48

Table 4. Two-group cross sections for the uranium isotopes in the fuel compact (5.2 w% enrichment) in the radial zones B, C, and D.

nuclide	ν		σ_{fis} (b)		σ_{capt} (b)		
	group 1	group 2	group 1	group 2	group 1	group 2	
^{235}U	B	2.438	2.438	11.18	302.3	6.000	51.94
	C	2.438	2.438	11.92	311.1	6.469	53.44
	D	2.439	2.438	10.93	313.0	5.846	53.72
^{238}U	B	2.742	2.489	5.486 E-2	6.640 E-6	2.661	1.544
	C	2.741	2.489	4.884 E-2	6.805 E-6	2.880	1.581
	D	2.742	2.489	5.667 E-2	6.841 E-6	2.595	1.589

Table 5. Two-group cross sections for the non-fissionable nuclides in the fuel compact (5.2 w% enrichment) in radial zones B, C, and D.

nuclide	σ_{tot} (b)		σ_{abs} (b)		σ_{fis} (b)		
	group 1	group 2	group 1	group 2	group 1	group 2	
O	B	3.807	3.775	1.543 E-3	1.063 E-4	3.350	3.620
	C	3.814	3.773	1.371 E-3	1.090 E-4	3.394	3.620
	D	3.805	3.773	1.590 E-3	1.096 E-4	3.351	3.619
Si	B	2.730	2.106	3.694 E-3	9.728 E-2	2.500	2.059
	C	2.672	2.108	3.707 E-3	9.978 E-2	2.455	2.059
	D	2.749	2.108	3.683 E-3	1.003 E-1	2.501	2.061
C	B	4.177	4.639	1.779 E-4	1.917 E-3	3.515	4.566
	C	4.220	4.636	1.647 E-4	1.966 E-3	3.609	4.568
	D	4.163	4.635	1.813 E-4	1.977 E-3	3.510	4.564
¹⁰ B	B	45.86	2177.5	43.47	2175.3	34.01	2199.1
	C	49.71	2233.4	47.33	2231.3	39.40	2201.1
	D	44.63	2245.6	42.23	2243.5	33.07	2266.9
¹¹ B	B	4.287	4.778	8.849 E-5	3.116 E-3	3.593	4.498
	C	4.332	4.778	9.315 E-5	3.197 E-3	3.690	4.497
	D	4.273	4.778	8.700 E-5	3.214 E-3	3.589	4.501

Table 6. Two-group cross sections for the nuclides in the graphite of the blocks in all radial zones

nuclide	σ_{tot} (b)		σ_{abs} (b)		σ_{fis} (b)		
	group 1	group 2	group 1	group 2	group 1	group 2	
C	A	4.290	4.810	1.178 E-4	2.185 E-3	3.442	4.772
	B	4.130	4.844	1.440 E-4	2.039 E-3	3.418	4.774
	C	4.183	4.846	1.351 E-4	2.095 E-3	3.528	4.776
	D	4.113	4.847	1.463 E-4	2.106 E-3	3.412	4.779
	E	4.347	4.815	1.161 E-4	2.580 E-3	3.500	4.786
	reflector	4.524	4.818	1.274 E-4	2.858 E-3	3.971	4.838
¹⁰ B	A	57.31	2483.0	54.99	2480.7	38.79	2600.2
	B	46.77	2316.6	44.43	2314.4	34.60	2344.3
	C	50.72	2380.7	48.40	2378.5	40.15	2345.5
	D	45.50	2393.3	43.16	2391.1	33.63	2424.5
	E	65.21	2933.7	62.91	2931.5	38.77	2788.0
	reflector	97.35	3251.3	95.12	3249.1	79.34	3168.6
¹¹ B	A	4.404	4.976	1.017 E-4	3.554 E-3	3.515	4.701
	B	4.239	4.995	8.824 E-5	3.316 E-3	3.495	4.705
	C	4.294	5.003	9.325 E-5	3.407 E-3	3.609	4.705
	D	4.221	5.004	8.666 E-5	3.425 E-3	3.490	4.718
	E	4.462	5.020	1.116 E-4	4.199 E-3	3.583	4.721
	reflector	4.640	5.052	1.519 E-4	4.654 E-3	4.066	4.755

Work Package: 1	HTR-N project document No.: HTR-N-02/09-S-1.1.2	Rev. 1
Task: 1.1&1.2	Document type: EC deliverable	

Cross sections for PANTHER

Cross sections for the reactor code PANTHER have been generated by means of the code suite WIMS-7B. Apart from service modules for group condensing and material homogenisation, two collision probability modules were used to calculate the flux weighted cross sections of the fuel cell (PROCOL) and for the fuel blocks or assemblies, control guide blocks and reflector blocks (PIJ).

General

In order to avoid much extra work, densities, impurities and sizes of graphite's, CFP's and coatings, weighted means of these parameters where appropriate, have been derived to be used all over the reactor.

This leads to the following standardised parameters for the CFP's:

	radius (μm)	density (g/cm^3)	material
fuel kernel	297.95	10.774	UO ₂
1st coating	358.80	1.127	PyC (low density)
2nd coating	389.45	1.896	PyC
3rd coating	418.35	3.225	SiC
4th coating	464.20	1.866	PyC

Compact dimensions: i/o diameter = 1.00/2.60 cm, height = 3.91 cm.

And for the graphite's:

	density (g/cm^3)	impurity (ppm B _{nat})
matrix	1.690	0.82
sleeve	1.770	0.37
fuel / control block	1.770	0.40
repl. reflector	1.760	0.37
perm. reflector	1.732	1.91

Work Package: 1	HTR-N project document No.: HTR-N-02/09-S-1.1.2	Rev. 1
Task: 1.1&1.2	Document type: EC deliverable	

PROCOL

In the WIMS-suite a cell module PROCOL, based on collision probabilities, exists to calculate fluxes in systems with spherical grains packed in a matrix with an annular geometry.

A cell radius of 3.29 cm has been used, consistent with a lattice of a 1/33rd part of a fuel block or assembly, in which explicitly modelled: the inner gas channel ($r=0.50$ cm), the compact ($r=1.30$ cm), the gas gap ($r=1.3125$ cm), sleeve ($r=1.70$ cm) and the fuel hole drilling in the fuel block ($r=2.05$ cm). Using this model, flux weighted cross sections are obtained for homogenised CFP's + matrix + gas gap, to form the compact material with cross sections in the 69 neutron energy groups structure of the library.

The spectrum in the centre of the inner gas channel in the compact with 5.2 w% enrichment is shown in fig. 1. Comparison with the spectrum as obtained with the KENO cross sections is very good. Differences are only due to the resolution of the spectrum with the number of energy groups used in the calculations (KENO: 172 vs. WIMS: 69).

Accordingly obtained cross sections were condensed to 16 neutron energy groups for subsequent use in the WIMS assembly module PIJ, which calculates collision probabilities in multi-pin assembly systems.

For comparison purposes microscopic cross sections for the nuclei present in the compacts were condensed to two group cross sections. In WIMS only microscopic absorption and fission cross sections are easily available, but for some elements transport and total cross sections could be deduced from macroscopic cross sections. Values for an enrichment of 5.2 w% are given in the tables below and can be compared with those values given in tables 1 and 2. Agreement is in general rather good which can be confirmed by the spectrum comparison of fig. 1 and the calculated neutron multiplication factors: $k_{inf} = 1.499$ for the 'KENO'-cell and $k_{inf} = 1.493$ for the 'PROCOL'-cell.

nuclide	$\sigma_{tot}(b)$		$\sigma_{abs}(b)$		$\sigma_{tr}(b)$	
	group 1	group 2	group 1	group 2	group 1	group 2
¹⁰ B			42.20	2095		
C	4.086	4.805	1.882E-4	1.856E-3	3.348	4.702
O			1.527E-3	1.029E-4		
Si			3.623E-3	9.397E-2		
²³⁵ U			1.692E+1	3.397E+2		
²³⁸ U			2.747	1.499		

	ν		$\sigma_{fis}(b)$		$\sigma_{capt}(b)$	
	group 1	group 2	group 1	group 2	group 1	group 2
²³⁵ U	2.438	2.438	1.096E+1	2.897E+2	5.968	49.91
²³⁸ U	2.742	2.489	5.768E-2	6.437E-6	2.689	1.499

Work Package: 1	HTR-N project document No.: HTR-N-02/09-S-1.1.2	Rev. 1
Task: 1.1&1.2	Document type: EC deliverable	

PIJ

For modelling in PIJ the fuel assembly has been adapted in the following way:

1. The stack of compacts has been moved to the top such that the upper rim of the upper compact is flush with the fuel block,
2. The upper graphite plug and buffer plate has been moved to the bottom,
3. The stack with the burnable poison (BP) pellets and graphite disks has been moved to the top as in 1, while the length of the upper section of the BP stack has been changed from 20 cm to 15 cm and the lower section to 25 cm
4. The fuel handling hole has been simplified by taking an effective diameter of 4.017 cm and a length of 25.0 cm.

This way four layers in the assembly can be created (fig. 2):

1. First layer of 15 cm height with compacts, fuel handling hole (FHH) and BP pellets,
2. Second layer of 10 cm with compacts, FHH and graphite disks,
3. Third layer of 25 cm with compacts, graphite for FHH and with BP pellets,
4. Fourth layer of remaining 8 cm with a mix of 4.75 cm of compact, 2.35 cm of graphite and 0.9 cm of void at the fuel positions and graphite at the FHH and BP positions.

Void has been modelled in the empty BP insertion leg.

For each layer a model of the fuel assembly has been laid out in which the hexagonal perimeter has been replaced by an equivalent circle (radius 19.01 cm). Within this circle the fuel positions (comprising: inner gas space, compact, sleeve and outer gas space), FHH and BP insertion holes are modelled at the exact positions and filled with the materials in conformance.

This circle in turn is surrounded by another circle (radius 38.01 cm), divided into 12 segments, to accommodate the matching surrounding materials for the fuel assembly under study (fig. 3).

It makes a total of 206 material regions per assembly layer.

The coolant bearing reflector blocks in the 1st, 2nd and 8th reactor layer are modelled in the same way but with empty fuel holes and of reduced diameter.

To reduce the number of materials, the PIJ model is finally divided into seven regions: one central region comprising the FHH position and the six inner fuel positions, and the six surrounding segments (fig. 3). Materials within a region are homogenised or smeared to one material. Finally the seven materials for the four layers are smeared, according to their height, to seven final materials for one assembly having flux weighted cross sections in 16 neutron energy groups.

The procedure for the control guide blocks (fig. 3) and reflector blocks is similar; also divided into seven regions but with only two layers, with and without FHH.

Work Package: 1	HTR-N project document No.: HTR-N-02/09-S-1.1.2	Rev. 1
Task: 1.1&1.2	Document type: EC deliverable	

Advantage of the sub-division in seven regions is that the anomalies in a block, like BP stacks, absent fuel pins, control guide holes, control rods, etc. are confined to only one region a piece and are not smeared over the entire block. This allows for more pronounced local absorption and/or streaming, which form major problems for modelling this kind of reactor cores.

For all 48 different block configurations (enrichments, block types, surroundings, etc.) two runs with PIJ were done; first a run without control rods (unrodded) and a second run with control rod material modelled in the control guide holes and using rodded material in that sector of the surrounding where present (rodded).

Afterward all cross sections were condensed to two energy groups ($E_{th} = 2.1$ eV) and organised in such a way that it can be used in the reactor code PANTHER, leading to 336 different materials in as well a rodded state as an unrodded state.

By making use of the modules PROCOL and PIJ the double heterogeneity formed by the CFP's and the fuel rods has been modelled explicitly and therefore no Dancoff factor has to be introduced.

Work Package: 1	HTR-N project document No.: HTR-N-02/09-S-1.1.2	Rev. 1
Task: 1.1&1.2	Document type: EC deliverable	

ANALYSIS OF THE SIMPLE CORE WITH KENO

Model of the HTTR

Two models of the HTTR have been developed. The first model is a very detailed model of the HTTR in which practically all components are modelled explicitly, with the following exceptions:

- 1 As mentioned before, the coated fuel particles were homogenised with the graphite matrix of the fuel compacts.
- 2 Conical shapes (upper part of fuel handling hole, control rod insertion hole in layer 6 (figure 5.2-2 of ref. 1), and reserve shutdown pellet insertion hole in control rod guide blocks in layer 7 (figure 5.2-3)) can not be modelled in KENO and are therefore approximated by cylinders with radii that preserve the volumes.
- 3 It also turned out to be impossible to model hexagonal blocks in KENO-Va. Therefore, the permanent reflector was approximated by a cylinder of 429.96 cm diameter which preserves the volume of the actual reflector. Furthermore, the hexagonal blocks in the core and in the replaceable reflector were represented by cylinders of 36 cm diameter (the distance between the parallel faces of the blocks). These cylinders (which contain all fuel rods and the two burnable poison rods or all coolant channels) were placed in a large cylinder of graphite (with a radius of 162.9 cm). Hence, in this way only the small gaps (2 mm on average) between the blocks are not represented explicitly.

Further details of this detailed KENO model can be found elsewhere [2]. The second model is identical to the 2D BOLD VENTURE model, which is described in section 4.1. It is referred to as the homogenised core model.

Results

Three runs with KENO have been performed for the simple core configuration (all fuel blocks contain 5.2% enriched uranium):

- 1 with the detailed model
- 2 with the detailed model in which the burnable poison rods have been replaced by graphite rods
- 3 with the homogenised core model

Each run comprised the simulation of 200 batches of 10000 histories each. The results are summarised in table 7.

Table 7. KENO results for the simple core

run	k_{eff}
detailed model	1.1278±0.0005
detailed model, BP rods replaced by C	1.3252±0.0005
homogenised model	1.3592±0.0005

The second run was performed to determine the reactivity worth of the BP rods as being $\Delta k = -0.1974$. Note that in the homogenised model the BP rods are not taken into account. Hence, the difference between the second and third run ($\Delta k = 0.0340$) can be attributed to the homogenisation of the core region, in particular to the lack of streaming.

Work Package: 1	HTR-N project document No.: HTR-N-02/09-S-1.1.2	Rev. 1
Task: 1.1&1.2	Document type: EC deliverable	

ANALYSES OF THE SIMPLE CORE WITH BOLD-VENTURE

Model of the HTTR

The HTTR was represented by an R-Z model. It contains six zones in the radial direction, and nine in the axial direction, one for each layer. The six radial zones are:

1. the central control rod guide column (column A)
2. the first fuel zone (the six B columns)
3. the second fuel zone (the 12 C columns: 6 fuel and 6 control rod columns)
4. the third and fourth fuel zone (the 18 D columns)
5. the replaceable reflector (the 24 E columns)
6. the permanent reflector

The height of each layer is 58 cm, except layer 9 (42.9 cm). The radii of the zones can be found in section 2.2.1. The atomic densities in the homogenised zones can be found in the appendix. Indeed, these densities have also been used in the last step of the cross-section generation procedure. Note that the 10 cm difference in height between fuel columns and control rod guide columns was ignored, and that the BP rods are not taken into account.

Results

Calculations were performed with a 2 cm mesh, both in axial and radial direction. A calculation requires about 3.5 minutes CPU time. The multiplication constant was found to be 1.3567, which is only 0.0025 lower than the corresponding value calculated with KENO. In order to represent the BP rods, the ^{10}B density in radial zones B, C, and D has been increased till $\Delta k = -0.1974$ was obtained (the reduction determined with the detailed KENO model), or to $k_{\text{eff}} = 1.1593$. The increase in the ^{10}B density in zone C was half of that in zones B and D, as only six of the 12 C-columns are fuel columns, whereas all B and D columns are fuel columns. The required ^{10}B density turned out to be $4.00 \cdot 10^{-7} \text{ 1/(b.cm)}$ (Note that the BP rods cannot simply be homogenised with the rest of the fuel block as this homogenisation would not take into account the self-shielding in the rods). The axial and radial distribution of the fast and thermal neutron flux is shown in figures 4 and 5, along with the corresponding fluxes in the fully loaded core.

KENO calculations have shown that the homogenisation leads to an over-estimation of k_{eff} by 0.0340. The reason is that the neutron streaming in the cylindrical and annular holes in the core region is not taken into account by the homogenisation. In diffusion theory, this enhanced streaming can be taken into account by adjusting the diffusion coefficient. Therefore, the diffusion coefficients in the five inner radial zones and the upper eight axial zones was multiplied by a modification factor. The value of this factor that yielded a reduction in k_{eff} of 0.0340 was determined to be 1.445. Note that this is just a first attempt to deal with the neutron streaming in diffusion theory calculations with BOLD VENTURE.

Work Package: 1	HTR-N project document No.: HTR-N-02/09-S-1.1.2	Rev. 1
Task: 1.1&1.2	Document type: EC deliverable	

ANALYSIS OF THE SIMPLE CORE WITH PANTHER

Model of the HTR

For PANTHER a 3-D model has been developed in a hexagonal representation, taking a cluster of seven sub hexes (size: 13.68 cm flat-to-flat) per hexagonal reactor assembly position in the radial direction and 5 layers per assembly in the axial direction. This leads to 937 radial reactor channels with an equivalent radius of 220 cm and 45 axial layers of 11.6 cm (fig. 6). The bottom of the control rod insertion holes has been taken flush with the top of the lowest fuel column block (58 cm level from the bottom, refer to fig. 25 of ref. 1) and the bottom of the shutdown hole has been taken flush with the top of the second block (116 cm level), just as for the irradiation holes. The widening of the control rod holes coincides with halfway the fourth block (203 cm level).

Control rods, those left partially inserted in the E-column ring, reached only till the bottom level of the upper block (464 cm level).

Materials defined and prepared in the WIMS data generation phase has been laid down according to proper compositions and orientations of the reactor assembly blocks in the reactor. For the simple core all enrichments were set at 5.2 w% and all burnable poison was taken as type H-II.

Results

The reactor was supposed to be at an overall temperature of 300 K and ran at very low power, so no Xe has been built up. Calculations resulted, after 75 seconds of CPU time also on a DEC- α , in a neutron multiplication factor of 1.1251, this is to be compared with the detailed KENO calculation, with neutron streaming, which yielded: $k_{\text{eff}} = 1.1278$. So this indicates that in the used WIMS and PANTHER models streaming effects have been properly accounted for.

The axial flux distributions of as the fast and thermal fluxes on the axis of the reactor are shown in figure 4. A slight asymmetry in these curves can be explained by the widening of the control rod guide holes down from the 203 cm level. More pronounced peaking of the thermal flux for the BOLD-VENTURE calculations can be attributed to the finer meshing in these calculation and by the zonal homogenisation of the voids and thus eliminating the streaming in the axial direction which results in a reduced penetration of the fast flux into the upper (UAR) and lower (LAR) axial reflectors.

Plots of the radial flux distributions at half core height can be seen in figure 7. The position of the fuel blocks, control rod blocks and reflectors are clearly visible in figure 7 by the peaking of the fast and thermal flux respectively. Due to the more detailed geometry in the PANTHER model, no representation of an averaged radial distributions as in figure 5 has been made.

Work Package: 1	HTR-N project document No.: HTR-N-02/09-S-1.1.2	Rev. 1
Task: 1.1&1.2	Document type: EC deliverable	

ANALYSIS OF THE FULLY LOADED CORE WITH BOLD-VENTURE

The analysis of the fully loaded core with the Monte Carlo code KENO-Va has been described in detail in a previous report [2]. Therefore, only the results obtained with the diffusion code BOLD VENTURE will be presented here.

Model of the HTTR

The model of the fully loaded core is basically identical to that of the simple core configuration. In this case, the atomic densities have been calculated for each horizontal layer, whereas in the simple configuration the densities in the core (layers 3 to 7) are assumed to be identical. This is true as far as the fuel blocks are concerned, but is not strictly true for the zones which contain control rod guide columns. Note also that for the simple core, each step in the cross-section generation procedure has to be executed only once. However, for the fully loaded core, step 1 must be repeated 12 times (one run for each enrichment), step 2 only once, steps 3, 4 and 5 12 times. Step 6 finally, was repeated 5 times, one for each layer in the core region. The five produced libraries in ISOTXS format were then combined to one large library (using an option provided by BOLD VENTURE). For the cross sections in layers 8 and 9 the cross sections for the permanent reflector from the ISOTXS library for layer 7 were used. Similarly, for layers 1 and 2 the cross sections for the permanent reflector from layer 3 were used. The atomic densities for each zone can be found in the appendix.

Results

As can be found in ref. 2, for the simple core, first a run was performed with the very detailed KENO model in which the BP rods were replaced by graphite rods, in correspondence with the homogenised model. The results are listed below and show that the reactivity effect of the BP rods is $\Delta k = 0.1775$.

Table 8. Analysis with KENO (from ref. 2).

run	k_{eff}
detailed model, BP rods replaced by C	1.3375±0.0005
detailed model, control rods withdrawn	1.1600±0.0005
detailed model, control rods inserted (406 cm)	0.6983±0.0005

The BOLD VENTURE model yielded $k_{\text{eff}} = 1.3750$ or $k_{\text{eff}} = 1.1975$, if corrected for the BP rods reactivity effect, which is 0.0375 higher than the multiplication constant obtained with the detailed KENO model, and can be attributed to the homogenisation of the core region. As for the simple core, the effect of the BP rods is taken into account in the homogenised model by increasing the ^{10}B density in all zones containing fuel blocks. No distinction is made between BP rods of type H-I or type H-II. The effective density was determined as $3.94 \cdot 10^{-7} \text{ 1/(b.cm)}$. The axial and radial distribution of the neutron flux is shown in figures 4 and 5. Some remarks about these figures are:

Work Package: 1	HTR-N project document No.: HTR-N-02/09-S-1.1.2	Rev. 1
Task: 1.1&1.2	Document type: EC deliverable	

1. In the fully loaded core the axial distribution is peaked in the upper part of the core because there the enrichment is maximal. The axial flux distribution in the simple core is almost symmetrical around the half core height. Almost, because the graphite densities in the upper and lower reflector are not equal (different control rod holes).
2. In the first radial zone (zone A) there is no fuel, only graphite. The same applies to zone E and of course to the permanent reflector. This explains why the thermal flux increases, and the fast flux decreases compared to those in zones B and D.
3. Radial zones B, C, and D contain fuel. However, whereas zones B and D only contain fuel, zone C also contains control rod guide blocks. This explains why the fast flux has maxima in zones B and D, and why the thermal flux has minima in these zones.

The final goal now is to compute the generation time and the effective fraction of delayed neutrons in a critical system, because these parameters can be measured and are of importance for kinetic experiments. It is assumed that the system is made critical as described in the benchmark documentation [1]. From the analysis with the detailed KENO model, it is known that the critical insertion depth is 234.5 cm [2], and the reactivity effect of this insertion is $-16.0\% \Delta k$. This insertion is almost 4 layers (232 cm). Hence, to represent the inserted rods in the critical state, the ^{10}B density in layers 1-4 was increased in radial zones A, C, and E until this resulted in $\Delta k = -0.16$. In fact, the ^{10}B atomic density was calculated according to:

$$N_{\text{B}10}^{(x)} = N_{\text{B}10}^{(x)}(0) + \text{DF}^{(x)} N_{\text{B}10}^{(\text{CR})}$$

where the superscript x indicates the radial zone and $\text{DF}^{(x)}$ is the so-called density factor for zone x. This factor accounts for the variation of the number of control rods relative to the volume of the zone. The values for DF in the 3 radial zones are listed in table 9.

Table 9. The density factor DF for the radial zones

zone	# rods	total # columns	DF
A	2	1	2
C	12	12	1
E	18	24	3/4

It turned out that in order to achieve a reduction of 0.16 in k_{eff} , $N_{\text{B}10}^{(\text{CR})}$ must be set to $2.7 \cdot 10^{-6} \text{ 1/(b.cm)}$. The resulting value of k_{eff} was 1.0378 (not unity because the neutron streaming effect has not been taken into account yet). The system was subsequently forced to criticality by increasing the diffusion coefficient in layers 1-8, radial zones A-E. The modification factor necessary turned out to be 1.367. The flux and the adjoint function were calculated and used in the first-order perturbation theory code PERT-V [4] to compute the generation time Λ and the effective fraction of delayed neutrons β_{eff} . Use was made of delayed neutron data for ^{235}U and ^{238}U from the JEF-1.1 library. The generation time was calculated to be 1.1064 ms, somewhat smaller than the generation time at critical calculated by KENO (1.2992 ms). The effective fraction of delayed neutrons was found to be $7.05 \cdot 10^{-3}$. Substituting the delayed neutron data of ^{235}U (relative abundance's and decay constants) and the calculated reduced generation time $\Lambda/\beta_{\text{eff}}$ into the inhour equation, the prompt decay constant α_0 (a directly measurable quantity) at critical can be calculated. The calculated values are listed in table 10.

Work Package: 1	HTR-N project document No.: HTR-N-02/09-S-1.1.2	Rev. 1
Task: 1.1&1.2	Document type: EC deliverable	

Table 10. Calculated kinetics parameters and the prompt decay constant at critical.

parameter	KENO	BOLD VENTURE / PERT-V
$\beta_{\text{eff}} \times 10^3$	7.051	
Λ (ms)	1.2992	1.1064
$\beta_{\text{eff}}/\Lambda$ (s ⁻¹)	5.43	6.37
α_0 (s ⁻¹)	6.03	6.94

Work Package: 1	HTR-N project document No.: HTR-N-02/09-S-1.1.2	Rev. 1
Task: 1.1&1.2	Document type: EC deliverable	

ANALYSIS OF THE FULLY LOADED CORE WITH PANTHER

Model of the HTR

The model of the fully loaded core is as far as the geometry and materials are concerned identical with that of the simple model, except that now all different enrichments and burnable poisons have been included.

In PANTHER the assemblies that carry control rods are represented by two sets of nuclear data: one set for the part where is no control rod inserted (unrodded) and a set for the rodded part. The control rod insertion depth for a certain control rod bank determines whether PANTHER uses the set for the rodded material or for the unrodded material in a particular mesh.

For symmetry purposes the central control rod block has been modelled with three rods instead of two but with reduced diameter (2/3rd), this to keep the viewing solid angle similar to two rods.

Because of the rather long diffusion length of the neutrons in a graphite reactor, the nuclear data of the neighbouring assemblies, despite their geometric separation, are highly influenced by the rod insertion in a control rod block. Therefore the core, here comprising all A to E columns, has been declared to be one control rod bank and thus all these blocks have rodded and unrodded data as already pointed out in Section 2.3.3.

PANTHER has a module to perform a critical control rod insertion search in which, on an iterative way, the control rod setting or insertion is determined at which the reactor is just critical.

Results

Again the reactor was supposed to be at an uniform temperature of 300 K and at such a low power level to avoid Xe poisoning. The calculated multiplication factor yielded now: $k_{\text{eff}} = 1.1595$, to be compared with the KENO result of: $k_{\text{eff}} = 1.1600$. Again in good correspondence with the detailed calculations by KENO.

For a core with all operational control rods inserted (insertion depth; 406 cm) a neutron multiplication factor of $k_{\text{eff}} = 0.7510$ has been calculated, versus $k_{\text{eff}} = 0.6983$ as obtained in the detailed KENO calculation. This shows a higher control rod worth for the KENO model.

The critical control rod insertion was established by PANTHER at 244.5 cm from the top of the reactor (522 cm level), which compares well with the value of 235.5 cm as obtained by KENO, or 161.5 cm and 170.5 cm respectively above the bottom of the active core and is consistent with the higher control rod worth in KENO.

Results of the axial flux distributions of the fast and thermal flux along the axis of the reactor for the situation without control rods (unrodded) are shown in figure 4 (solid line) together with those of the simple core (dashed) and for both the PANTHER (ECN) and BOLD-VENTURE (IRI) results. This figure shows for both cores a less impounding thermal flux at the reflector-core interfaces in the PANTHER calculations. This is partially due to a coarser meshing in PANTHER but also to the better representation of the control rod guide holes in the PANTHER model, which gives rise to substantial axial



Work Package: 1	HTR-N project document No.: HTR-N-02/09-S-1.1.2	Rev. 1
Task: 1.1&1.2	Document type: EC deliverable	

streaming. In figure 8, a plot of the radial power density, at the unrodded half core position (unrodded), can be seen which shows a flatter power distribution than for the simple core (5.2 w%), indicating the importance of the enrichment distribution.

The plots of the radial thermal flux at half core height (unrodded and rodded in fig. 9) shows clearly the positions of the meshes with inserted control rods (thermal flux dips). Further plots of the axial and radial flux and power distributions are given in the figures 10 to 13, for the simple core (5.2 w%), the fully loaded core (unrodded) and its critical rod setting (critical). Axial (R-Z) distributions are obtained by averaging over the radial intervals with the same radius in a reactor layer, thus losing part of the radial structure.

Work Package: 1	HTR-N project document No.: HTR-N-02/09-S-1.1.2	Rev. 1
Task: 1.1&1.2	Document type: EC deliverable	

CONCLUSION

On the level of cell calculations good agreement has been found between the cross sections and spectra as prepared by the SCALE-system and as prepared by WIMS.

When performing diffusion calculations it is good custom to homogenise the materials in a reactor core after cell calculations because of the shortage of calculational dimensions and/or to reduce the number of spatial intervals to speed up the calculation time. But then in reactor systems with very distinct absorber pins and guiding holes one needs to tune the nuclear data on the basis of a Monte Carlo code like KENO capable of a more explicit geometry. Otherwise a more detailed geometry has to be used to account for the proper absorption and neutron streaming through the voids. When done in the latter manner, the PANTHER results are in very good agreement with the results of KENO with an exact geometric model.

Finally a summary of the main results for the different codes is given in table 11.

Table 11. Comparison of the results.

	KENO	BOLD-VENTURE	PANTHER
k_{eff} simple core	1.1278	1.1592	1.1251
k_{eff} fully loaded core			
- rods withdrawn	1.1600	1.1974	1.1595
- rods inserted	0.6983		0.7510
critical insertion			
- above bottom core	170.5 cm		161.5 cm
- from top reactor	235.5 cm		244.5 cm

Work Package: 1	HTR-N project document No.: HTR-N-02/09-S-1.1.2	Rev. 1
Task: 1.1&1.2	Document type: EC deliverable	

REFERENCES

- [1] M. Nakano et al., *Benchmark Problems of Start-up Core Physics of High Temperature Engineering Test Reactor (HTTR)*, JAERI-10-005, Japan (1998)
- [2] E.J.M. Wallerbos, J.E. Hoogenboom, *IRI Results for the benchmark problems of start-up core physics of the high temperature engineering test reactor (HTTR)*, IRI-131-98-007, Interfaculty Reactor Institute, Delft (1998)
- [3] E.J.M. Wallerbos, J.E. Hoogenboom and H. van Dam, *IRI results for LEU HTR-PROTEUS cores 5, 7, 9 and 10*, IRI-131-97-005, Interfaculty Reactor Institute, Delft (1997)
- [4] R.W. Hardie and W.W. Little, Jr., *PERT-V: A Two-Dimensional Perturbation Code for Fast Reactor Analysis*, Battelle-Northwest, Richland, Wash. Pacific Northwest Laboratory, Report BNWL-1162, (1969)
- [5] D. Mathews, *The PSI version of the PERT-V code*, TM-41-91-29, Paul Scherrer Institute, Switzerland (1991)

Work Package: 1	HTR-N project document No.: HTR-N-02/09-S-1.1.2	Rev. 1
Task: 1.1&1.2	Document type: EC deliverable	

FIGURES

CONTENTS

Figure 1: Neutron spectrum in the centre of the compact.

Figure 2: Axial composition of the fuel block in PIJ.

Figure 3: Radial composition of the fuel and control guide block in PIJ.

Figure 4: Axial flux distribution along the reactor axis in the simple core (dotted lines) and the fully loaded core (solid lines) with PANTHER (ECN) and BOLD VENTURE (IRI).

Figure 5: Radial flux distribution at the reactor midplane in the simple core (dotted line) and the fully loaded core (solid line) from BOLD VENTURE.

Figure 6: Radial composition of the PANTHER model.

Figure 7: Radial flux distribution at midplane core for the simple core from PANTHER.

Figure 8: Radial power density distribution at midplane core from PANTHER for the simple core (5.2 w%) and the fully loaded core (unrodded).

Figure 9: Radial distribution of the thermal flux at midplane core for the fully loaded core with inserted control rods (rodded) and without (unrodded).

Figure 10: Radial distribution of the fast and thermal flux at midplane core for the fully loaded core (unrodded).

Figure 11: Radially averaged axial fast flux distribution for the simple core (5.2 w%), fully loaded core (unrodded) and at critical control rod setting (critical) from PANTHER.

Figure 12: Radially averaged axial thermal flux distribution for the simple core (5.2 w%), fully loaded core (unrodded) and at critical rod setting (critical) from PANTHER.

Figure 13: Radially averaged axial power density distribution for the simple core (5.2 w%), fully loaded core (unrodded) and at critical rod setting (critical)

Work Package: 1	HTR-N project document No.: HTR-N-02/09-S-1.1.2	Rev. 1
Task: 1.1&1.2	Document type: EC deliverable	

Neutron spectrum

Centre compact

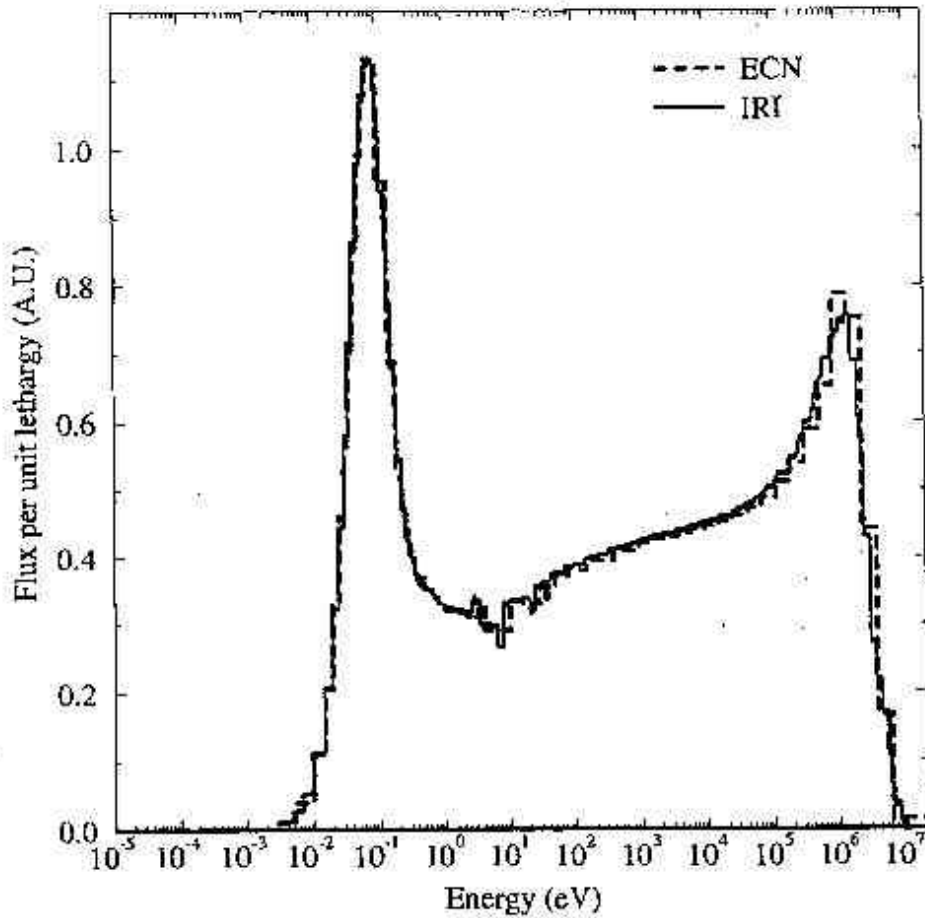


Figure 1: Neutron spectrum in the centre of the compact.

Work Package: 1	HTR-N project document No.: HTR-N-02/09-S-1.1.2	Rev. 1
Task: 1.1&1.2	Document type: EC deliverable	

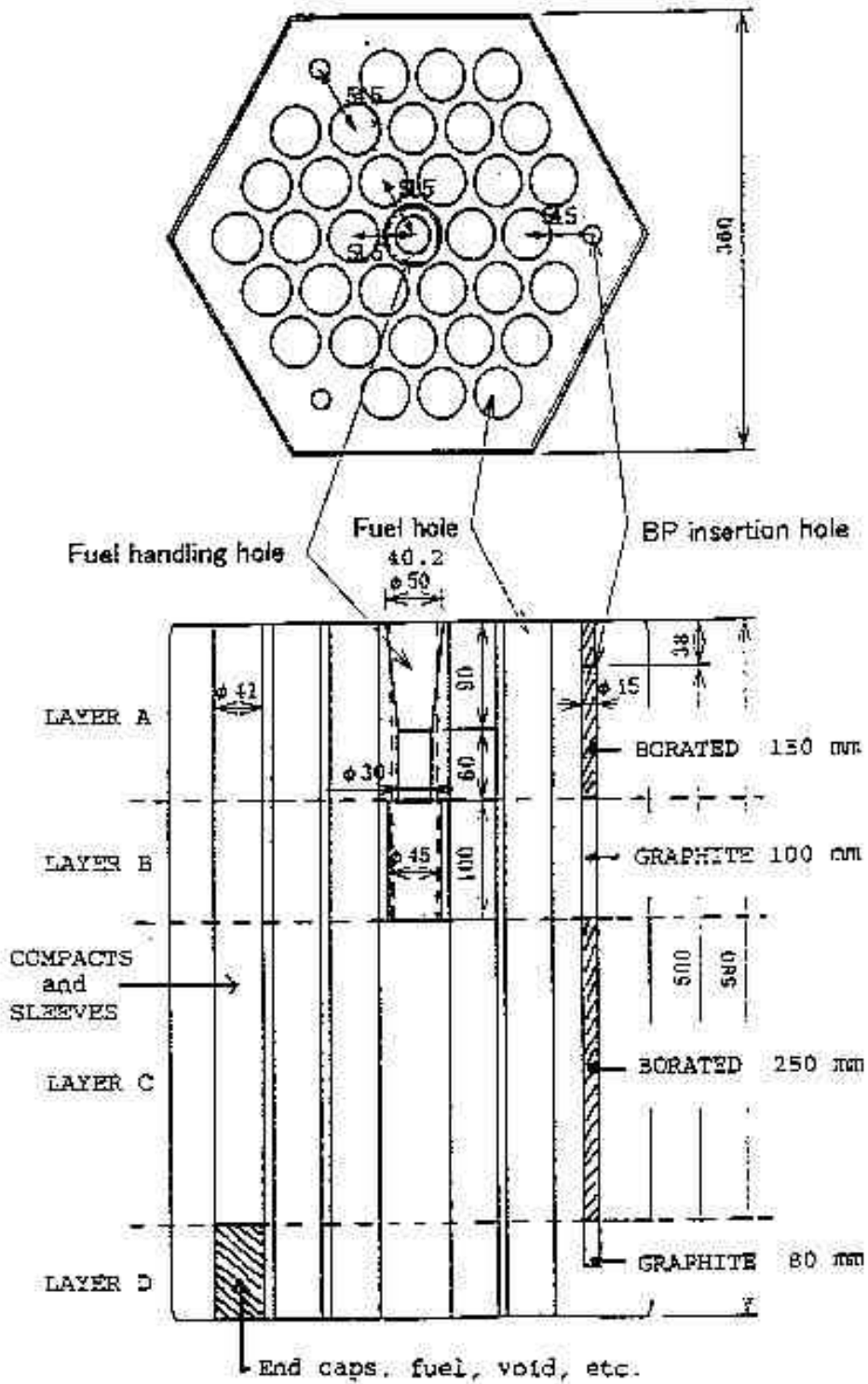


Figure 2: Axial composition of the fuel block in PIJ.

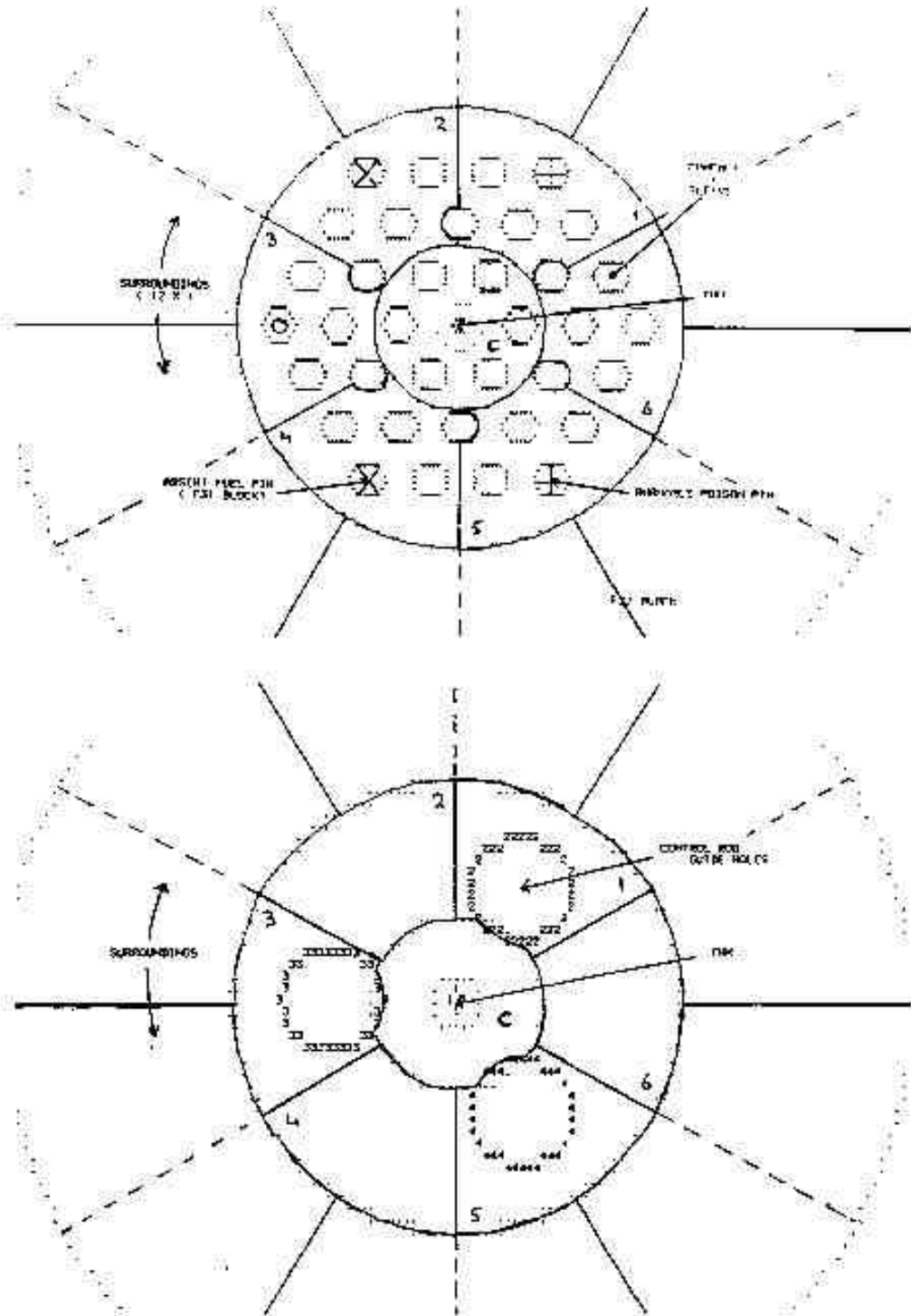


Figure 3: Radial composition of the fuel and control guide block in PIJ.

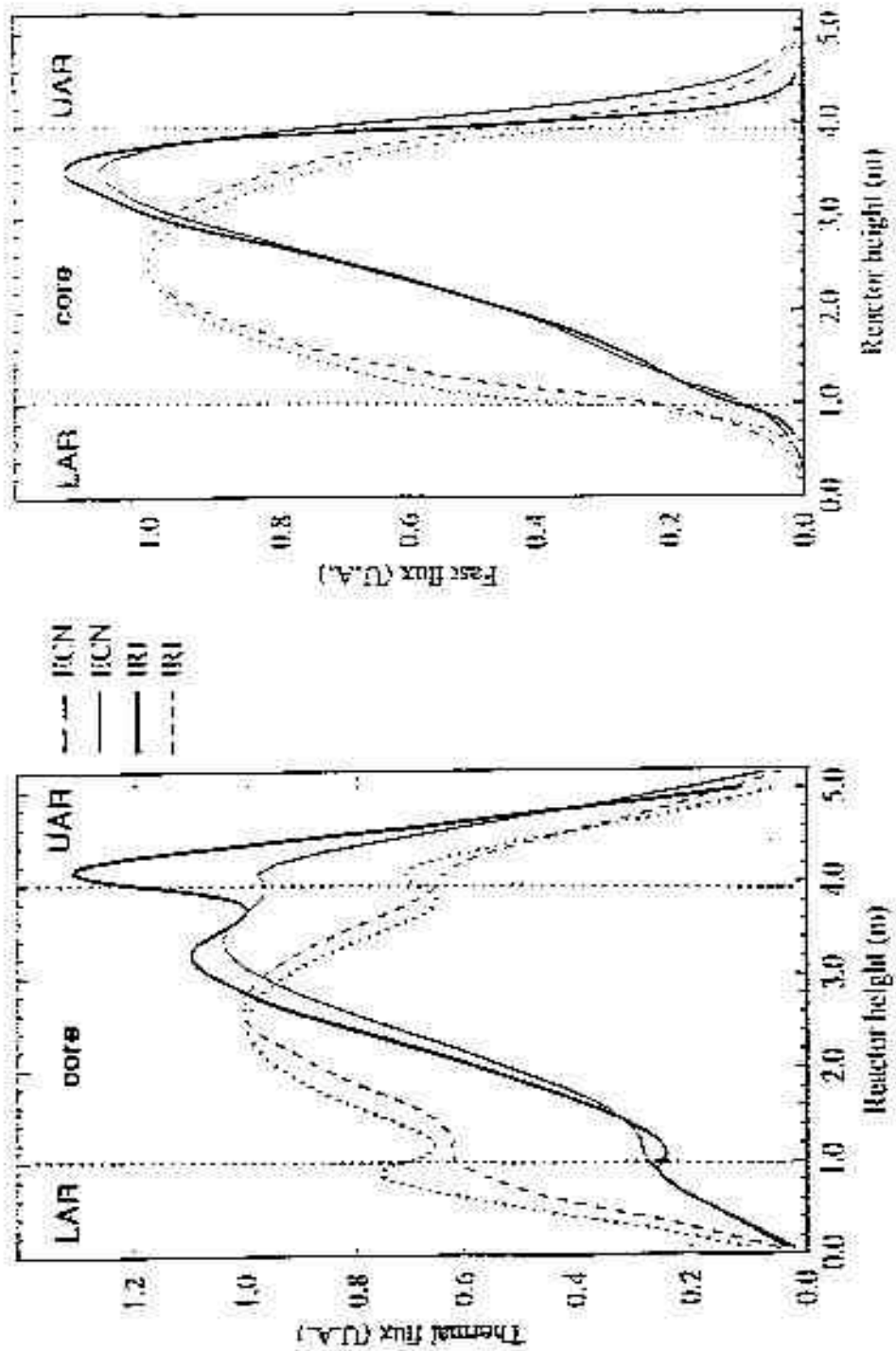


Figure 4: Axial flux distribution along the reactor axis in the simple core (dotted lines) and the fully loaded core (solid lines) with PANTHER (ECN) and BOLD VENTURE (IRI). LAR and UAR are the Lower and Upper Axial Reflectors.

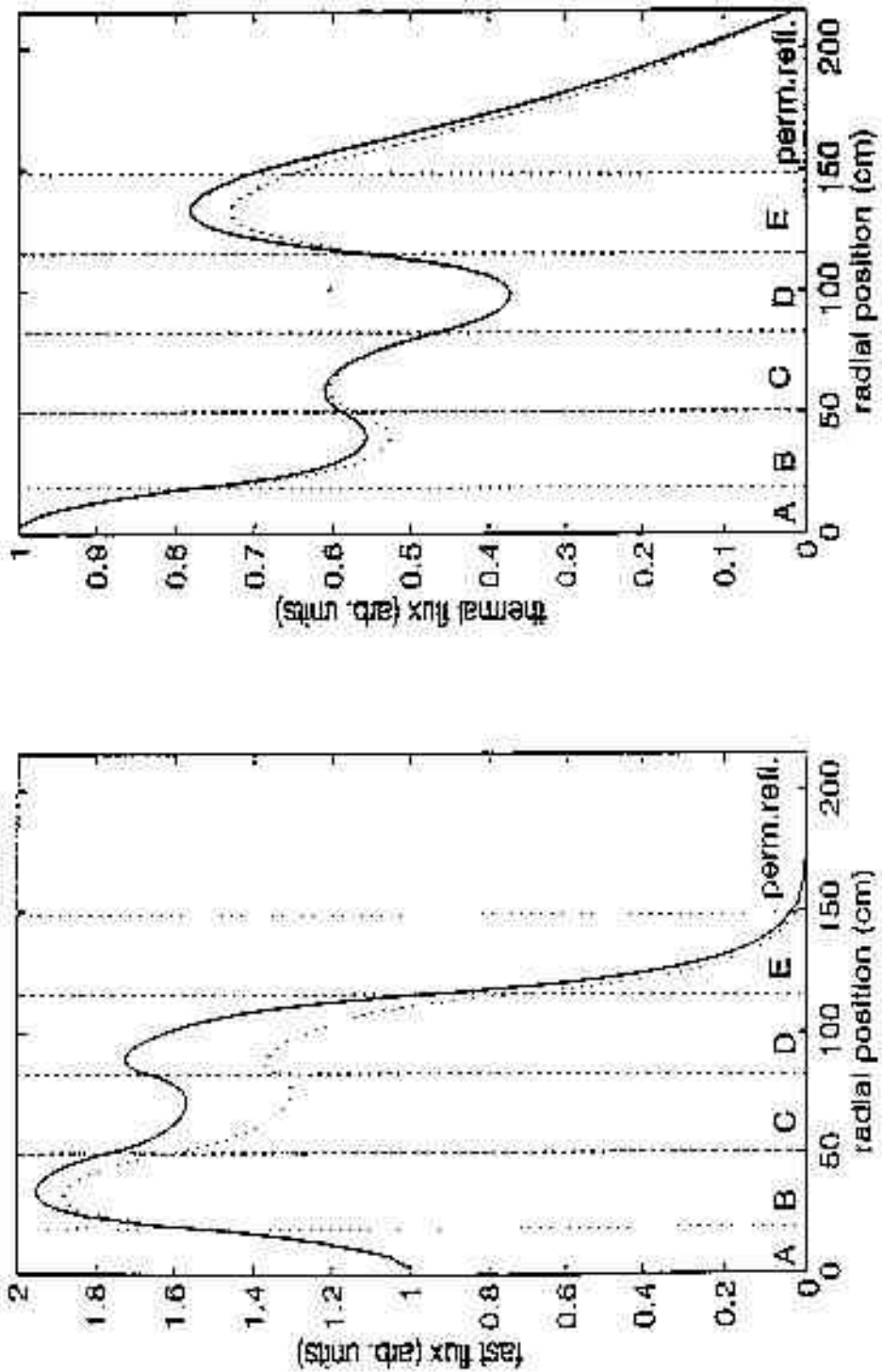


Figure 5: Radial flux distribution at the reactor midplane in the simple core (dotted line) and the fully loaded core (solid line).

Work Package: 1		HTR-N project document No.: HTR-N-02/09-S-1.1.2	Rev. 1
Task:	1.1&1.2	Document type: EC deliverable	

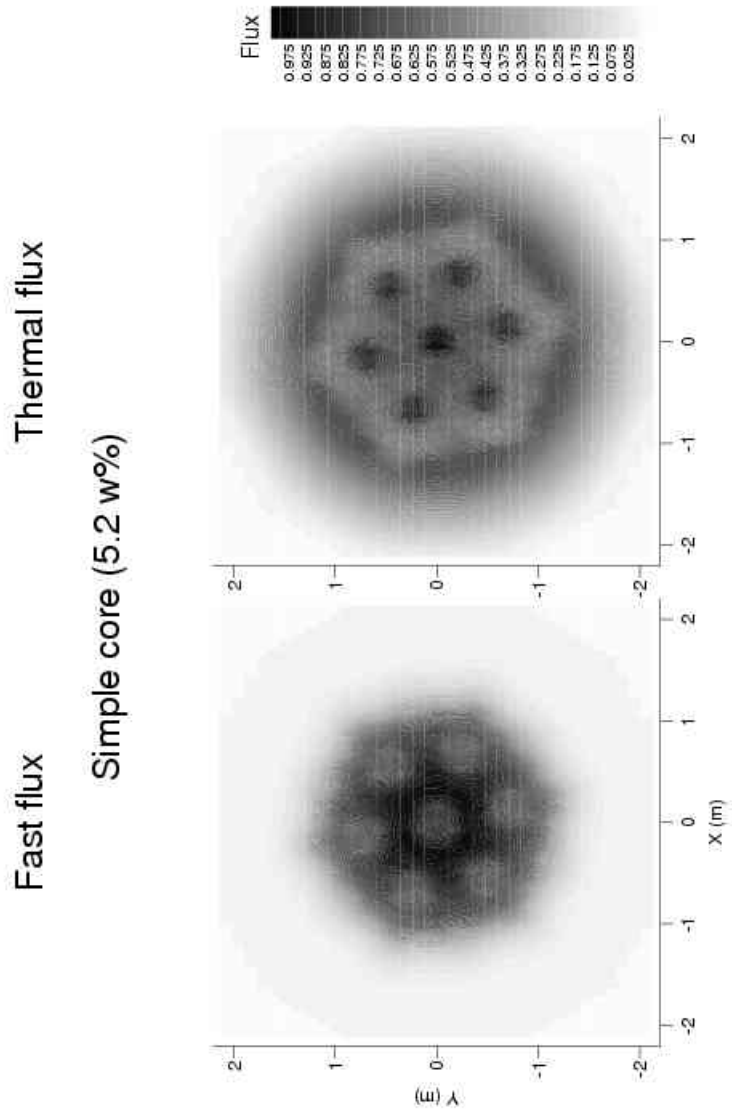


Figure 7: Radial flux distribution at midplane core for the simple core from PANTHER.

Work Package: 1		HTR-N project document No.: HTR-N-02/09-S-1.1.2	Rev. 1
Task:	1.1&1.2	Document type: EC deliverable	

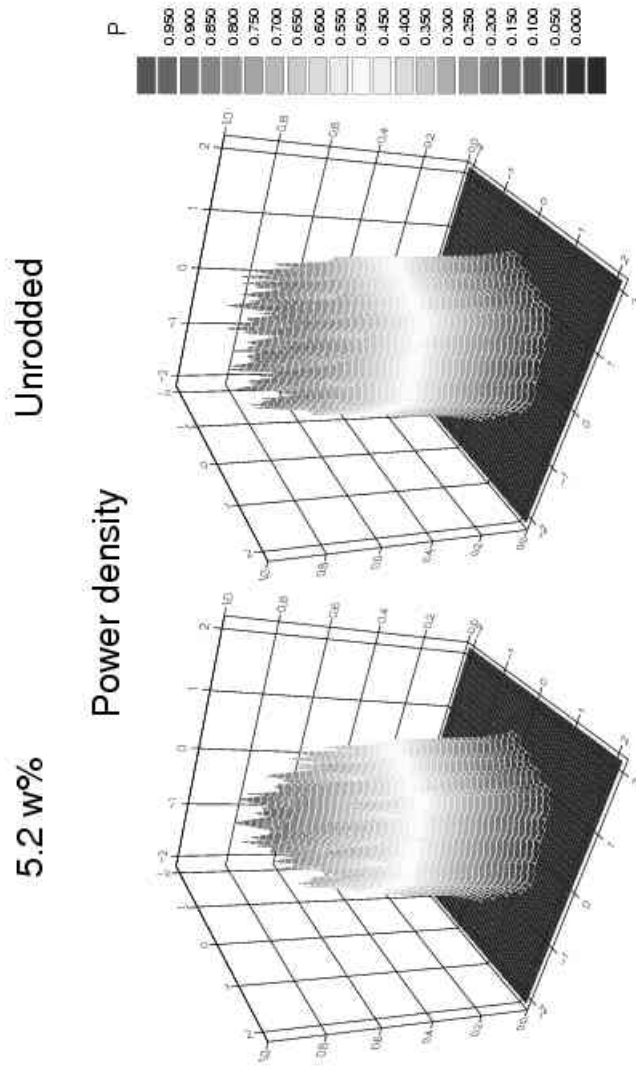


Figure 8: Radial power density distribution at midplane core from PANTHER for the simple core (5.2 w%) and the fully loaded core (unrodded).

Work Package: 1		HTR-N project document No.: HTR-N-02/09-S-1.1.2	Rev. 1
Task:	1.1&1.2	Document type: EC deliverable	

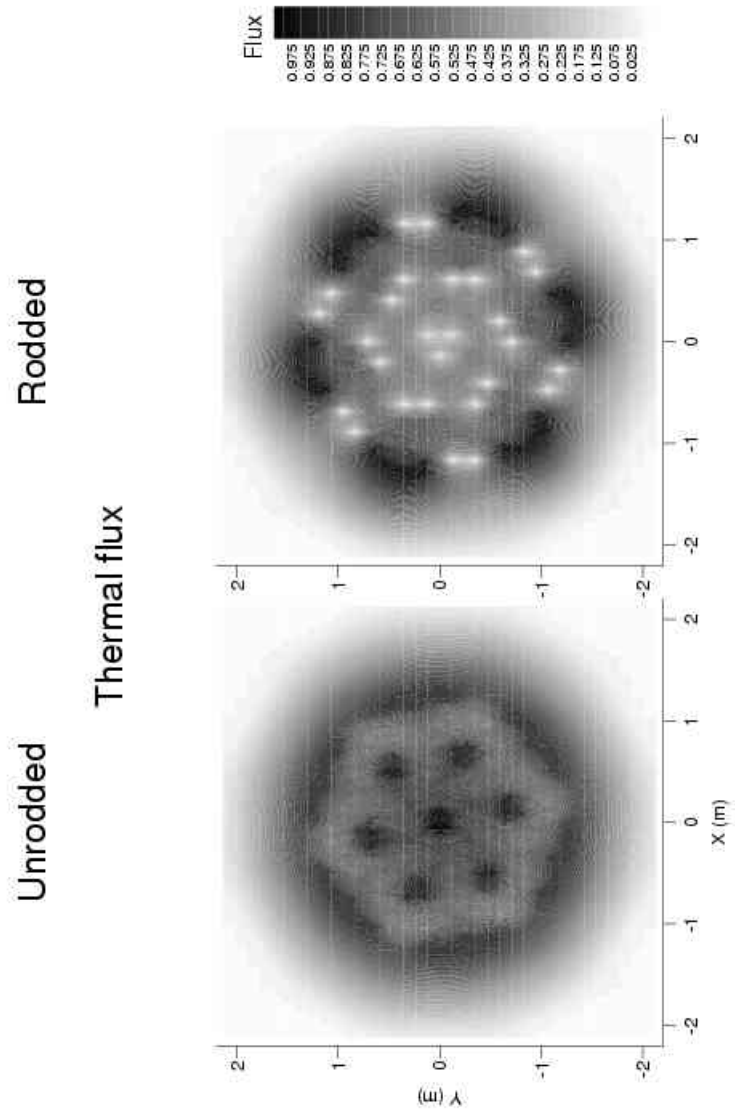


Figure 9: Radial distribution of the thermal flux at midplane core for the fully loaded core with inserted control rods (rodDED) and without (unrodDED).

Work Package: 1		HTR-N project document No.: HTR-N-02/09-S-1.1.2	Rev. 1
Task:	1.1&1.2	Document type: EC deliverable	

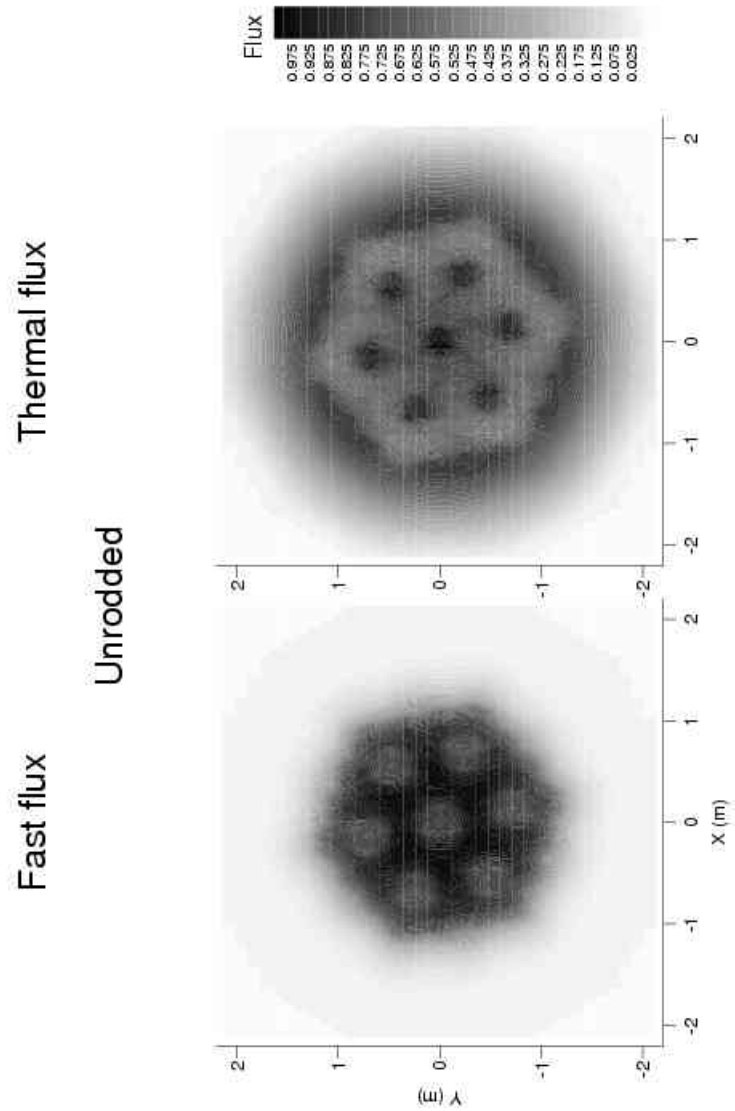


Figure 10: Radial distribution of the fast and thermal flux at midplane core for the fully loaded core (unrodded).

Work Package: 1		HTR-N project document No.: HTR-N-02/09-S-1.1.2	Rev. 1
Task:	1.1&1.2	Document type: EC deliverable	

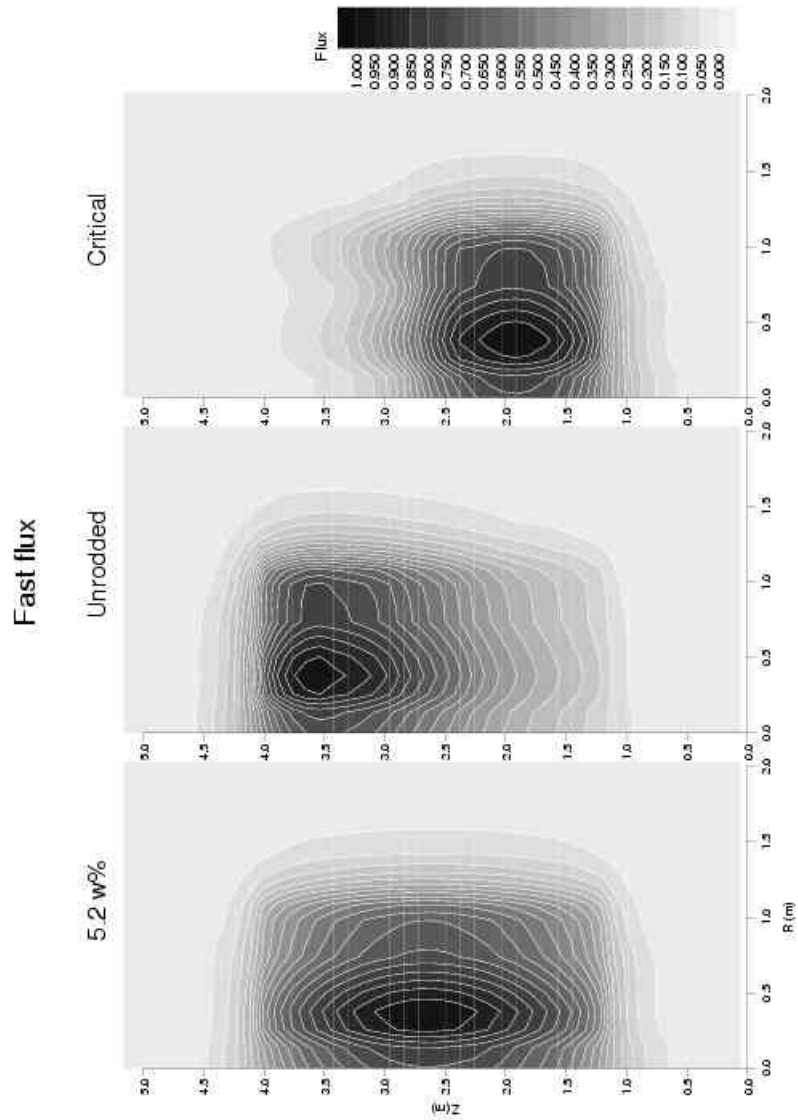


Figure 11:14 Radially averaged axial fast flux distribution for the simple core (5.2 w%), fully loaded core (unrodded) and at critical control rod setting (critical) from PANTHER.

Work Package: 1		HTR-N project document No.: HTR-N-02/09-S-1.1.2	Rev. 1
Task:	1.1&1.2	Document type: EC deliverable	

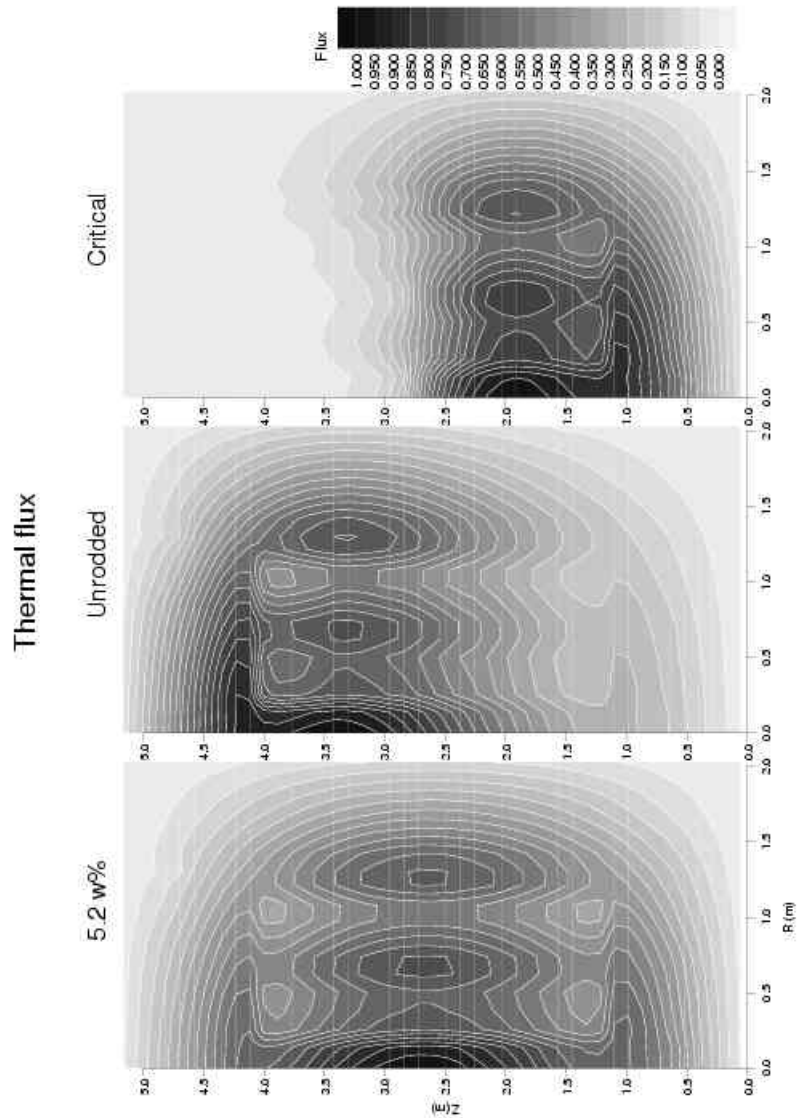


Figure 12: Radially averaged axial thermal flux distribution for the simple core (5.2 w%), fully loaded core (unrodded) and at critical rod setting (critical) from PANTHER.

Work Package: 1		HTR-N project document No.: HTR-N-02/09-S-1.1.2	Rev. 1
Task:	1.1&1.2	Document type: EC deliverable	

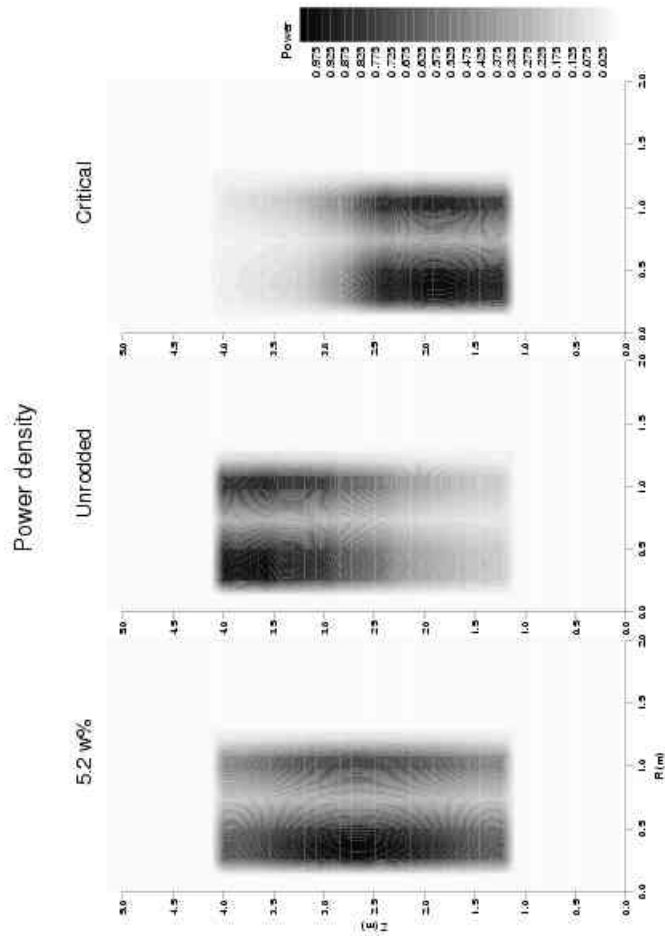


Figure 13: Radially averaged axial power density distribution for the simple core (5.2 w%), fully loaded core (unrodded) and at critical rod setting (critical).

APPENDIX

1 Atomic densities in the homogenised model.

In layers 1, 2, 8 and 9 first the density of the graphite is calculated by dividing the total mass of all blocks in the zone (which can be found in tables 5.2-2 to 5.2-19 in Ref. 1) by the zone volume. It is then straightforward to compute the carbon atomic density and the density of the boron. The helium is not taken into account.

In layers 3-7, the homogenised densities for the material within the fuel compacts is obtained by multiplying the densities of the fuel compact unit cell (see table A4 in Ref. 2) by a dilution factor for the zone of interest, which is given by

$$f = N_{\text{block}} N_{\text{rod}} V_{\text{rod}} / V_{\text{zone}} \quad (\text{A1})$$

where N_{block} is the number of fuel blocks in a zone, N_{rod} is the number of fuel rods per fuel block, V_{rod} is the volume of a fuel rod, and V_{zone} is the total volume of the zone. Table A1 summarises factors for zones B, C, and D. For zone D two numbers can be found, one for the fuel rods in fuel zone 3, and one for the fuel rods in fuel zone 4 (the fuel zone numbers are specified in figure 5.1-2 in Ref. 1). In case of the simple core, the fuel in fuel zones 3 and 4 are identical and hence the dilution factors can be added.

Table A1. Dilution factors for zones B, C, and D

zone	dilution factor	
B	0.123835	
C	0.0619175	
D	0.077553	0.038777

To obtain the carbon and boron atomic density of the fuel blocks, first the total carbon and boron mass in the zone are computed:

$$M_C = M_{\text{blocks}} + M_{\text{sleeves}} = N_{\text{block}} \rho_{\text{block}} (V_{\text{block}} - F_{\text{fhh}} - N_{\text{rod}} V_{\text{chan}}) + N_{\text{block}} N_{\text{rod}} \rho_{\text{sleeve}} V_{\text{sleeve}} \quad (\text{A2})$$

$$M_{\text{natB}} = I_{\text{block}} M_{\text{block}} + I_{\text{sleeve}} M_{\text{sleeve}} \quad (\text{A3})$$

where ρ_{block} is the density of the fuel block, V_{fhh} is the volume of the fuel handling hole (see Ref. 1), V_{chan} is the volume of a fuel rod channel, ρ_{sleeve} is the density of the fuel rod sleeve, V_{sleeve} the volume of the rod sleeve, I_{block} is the impurity of the block graphite, and I_{sleeve} is the impurity of the sleeve graphite. The values of these parameters can either be found in Ref. 1 or Ref. 2. Note that in zone C the mass of the control rod guide columns must be added to M_C . These masses are specified in Ref. 1. It is then straightforward to compute the atomic densities.

The atomic densities in the permanent reflector can be found in table A16 in Ref. 2.

1.1 The simple core

Table A2. Atomic densities in the zones of the homogenised model of the simple core

layer	isotope	A	B	C	D	E
1	C	5.96791E-2	7.64293E-2	6.80543E-2	7.72061E-2	7.31550E-2
	¹⁰ B	5.25175E-9	6.72575E-9	5.98876E-9	6.79411E-9	6.43761E-9
	¹¹ B	2.12722E-8	2.72427E-8	2.42575E-8	2.75196E-8	2.60756E-8
2	C	5.96791E-2	7.52106E-2	6.74450E-2	7.54999E-2	7.31550E-2
	¹⁰ B	5.25175E-9	6.61851E-9	5.93513E-9	6.64397E-9	6.43761E-9
	¹¹ B	2.12722E-8	2.68083E-8	2.40403E-8	2.69114E-8	2.60756E-8
3-7	²³⁵ U		1.24464E-5	6.22320E-6	1.24464E-5	
	²³⁸ U		2.24041E-4	1.12021E-4	2.24041E-4	
	O		4.72974E-4	2.36487E-4	4.72974E-4	
	Si		2.52147E-4	1.26073E-4	2.52147E-4	
	C		9.40767E-3	4.70384E-3	9.40767E-3	
	¹⁰ B		1.13291E-9	5.6646E-10	1.13291E-9	
	¹¹ B		4.58887E-9	2.29443E-9	4.58887E-9	
	C-block	5.80491E-2	6.32031E-2	6.06120E-2	6.32031E-2	7.26679E-2
	¹⁰ B-block	5.10830E-9	4.38391E-9	4.77766E-9	4.38391E-9	6.39475E-9
	¹¹ B-block	2.06912E-8	1.77571E-8	1.93519E-8	1.77571E-8	2.59020E-8
8	C	6.30687E-2	7.58809E-2	6.94749E-2	7.63530E-2	7.79604E-2
	¹⁰ B	5.55003E-9	6.67749E-9	6.11377E-9	6.71904E-9	6.86049E-9
	¹¹ B	2.24804E-8	2.70472E-8	2.47639E-8	2.72155E-8	2.77884E-8
9	C	6.73342E-2	6.98558E-2	6.86903E-2	6.98151E-2	7.50288E-2
	¹⁰ B	5.92539E-9	6.14729E-9	6.04473E-9	6.14370E-9	6.60251E-9
	¹¹ B	2.40008E-8	2.48996E-8	2.44842E-8	2.48851E-8	2.67435E-8

1.2 The fully loaded core

Table A3. Atomic densities in the zones of the homogenised model of the fully loaded core

layer / isotope	A	B	C	D	E		
1 C	5.96791E-2	7.64293E-2	6.80543E-2	7.72061E-2	7.31550E-2		
	¹⁰ B	5.25175E-9	6.72575E-9	5.98876E-9	6.79411E-9	6.43761E-9	
	¹¹ B	2.12722E-8	2.72427E-8	2.42575E-8	2.75196E-8	2.60756E-8	
2 C	5.96791E-2	7.52106E-2	6.74450E-2	7.54999E-2	7.31550E-2		
	¹⁰ B	5.25175E-9	6.61851E-9	5.93513E-9	6.64397E-9	6.43761E-9	
	¹¹ B	2.12722E-8	2.68083E-8	2.40403E-8	2.69114E-8	2.60756E-8	
3 ²³⁵ U		1.59828E-5	9.47053E-6	1.38494E-5	7.33430E-6		
	²³⁸ U		2.20425E-4	1.10226E-4	1.32451E-4	6.65772E-5	
	O		4.72816E-4	2.39392E-4	2.92601E-4	1.47823E-4	
	Si		2.52019E-4	1.27584E-4	1.55915E-4	7.87647E-4	
	C		9.39515E-3	4.72548E-3	5.88930E-3	2.95757E-3	
	¹⁰ B		8.0796E-10	7.0582E-10	9.0479E-10	4.5874E-10	
	¹¹ B		3.27265E-9	2.85890E-9	3.66487E-9	1.85812E-9	
	C-bl	5.96791E-2	6.32031E-2	6.13708E-2	4.31105E-2	2.15552E-2	7.31550E-2
	¹⁰ B-bl	5.25175E-9	4.38391E-9	4.81164E-9	2.99391E-9	1.49695E-9	6.43761E-9
	¹¹ B-bl	2.12722E-8	1.77571E-8	1.94896E-8	1.21268E-8	6.06340E-9	2.60756E-8
4 ²³⁵ U		1.24464E-5	7.47443E-6	1.07228E-5	5.93105E-6		
	²³⁸ U		2.24041E-4	1.10625E-4	1.36684E-4	6.90302E-5	
	O		4.72974E-4	2.36199E-4	2.94813E-4	1.49923E-4	
	Si		2.52147E-4	1.25905E-4	1.57132E-4	7.99013E-4	
	C		9.40767E-3	4.68932E-3	5.87318E-3	2.95940E-3	

HTR-N

Work Package: 1	HTR-N project document No.: HTR-N-02/09-S-1.1.2	Rev. 1
Task: 1.1&1.2	Document type: EC deliverable	

¹⁰ B		1.13291E-9	4.3542E-10	8.5926E-10	4.4203E-10	
¹¹ B		4.58887E-9	1.76366E-9	3.48044E-9	1.79043E-9	
C-bl	5.96791E-2	6.32031E-2	6.14412E-2	4.31105E-2	2.15552E-2	7.31550E-2
¹⁰ B-bl	5.25175E-9	4.38391E-9	4.81784E-9	2.99391E-9	1.49695E-9	6.43761E-9
¹¹ B-bl	2.12722E-8	1.77571E-8	1.95147E-8	1.21268E-8	6.06340E-9	2.60756E-8
5 ²³⁵ U		1.02922E-5	6.22320E-6	8.86497E-6	4.68096E-6	
²³⁸ U		2.26167E-4	1.12021E-4	1.39252E-4	6.92803E-5	
O		4.72920E-4	2.36487E-4	2.96234E-4	1.48054E-4	
Si		2.52143E-4	1.26073E-4	1.57912E-4	7.88496E-4	
C		9.40768E-3	4.70384E-3	5.89167E-3	2.93675E-3	
¹⁰ B		1.13292E-9	5.6646E-10	5.1692E-10	2.7269E-10	
¹¹ B		4.58889E-9	2.29443E-9	2.09378E-9	1.10452E-9	
C-bl	5.96791E-2	6.32031E-2	6.14412E-2	4.31105E-2	2.15552E-2	7.31550E-2
¹⁰ B-bl	5.25175E-9	4.38391E-9	4.81784E-9	2.99391E-9	1.49695E-9	6.43761E-9
¹¹ B-bl	2.12722E-8	1.77571E-8	1.95147E-8	1.21268E-8	6.06340E-9	2.60756E-8
6 ²³⁵ U		7.98178E-6	4.66739E-6	6.44562E-6	3.59756E-6	
²³⁸ U		2.30864E-4	1.13557E-4	1.41640E-4	7.04502E-5	
O		4.77691E-4	2.36448E-4	2.96172E-4	1.48096E-4	
Si		2.54715E-4	1.26071E-4	1.57908E-4	7.89547E-4	
C		9.42695E-3	4.70385E-3	5.89169E-3	2.94584E-3	
¹⁰ B		1.53719E-9	5.6646E-10	7.0951E-10	3.5475E-10	
¹¹ B		6.22639E-9	2.29445E-9	2.87386E-9	1.43692E-9	
C-bl	5.55584E-2	6.32031E-2	5.93808E-2	4.31105E-2	2.15552E-2	7.16097E-2
¹⁰ B-bl	4.88912E-9	4.38391E-9	4.63653E-9	2.99391E-9	1.49695E-9	6.30162E-9
¹¹ B-bl	1.98034E-8	1.77571E-8	1.87803E-8	1.21268E-8	6.06340E-9	2.55248E-8
7 ²³⁵ U		7.98178E-6	4.66739E-6	6.44562E-6	3.59756E-6	
²³⁸ U		2.30864E-4	1.13557E-4	1.41640E-4	7.04502E-5	
O		4.77691E-4	2.36448E-4	2.96172E-4	1.48096E-4	
Si		2.54715E-4	1.26071E-4	1.57908E-4	7.89547E-4	
C		9.42695E-3	4.70385E-3	5.89169E-3	2.94584E-3	
¹⁰ B		1.53719E-9	5.6646E-10	7.0951E-10	3.5475E-10	
¹¹ B		6.22639E-9	2.29445E-9	2.87386E-9	1.43692E-9	
C-bl	5.56498E-2	6.32031E-2	5.94265E-2	4.31105E-2	2.15552E-2	7.22647E-2
¹⁰ B-bl	4.89716E-9	4.38391E-9	4.64055E-9	2.99391E-9	1.49695E-9	6.35927E-9
¹¹ B-bl	1.98360E-8	1.77571E-8	1.87966E-8	1.21268E-8	6.06340E-9	2.57583E-8
8 C	6.30687E-2	7.58809E-2	6.94749E-2	7.63530E-2		7.79604E-2
¹⁰ B	5.55003E-9	6.67749E-9	6.11377E-9	6.71904E-9		6.86049E-9
¹¹ B	2.24804E-8	2.70472E-8	2.47639E-8	2.72155E-8		2.77884E-8
9 C	6.73342E-2	6.98558E-2	6.86903E-2	6.98151E-2		7.50288E-2
¹⁰ B	5.92539E-9	6.14729E-9	6.04473E-9	6.14370E-9		6.60251E-9
¹¹ B	2.40008E-8	2.48996E-8	2.44842E-8	2.48851E-8		2.67435E-8

HTR-N

Work Package: 1	HTR-N project document No.: HTR-N-02/09-S-1.1.2	Rev. 1
Task: 1.1&1.2	Document type: EC deliverable	
